MATHEMATICAL BIOSCIENCES
AND ENGINEERING
Volume **11**, Number **6**, December **2014**

doi:10.3934/mbe.2014.11.1247

pp. **1247–1274**

SPATIOTEMPORAL COMPLEXITY IN A PREDATOR–PREY MODEL WITH WEAK ALLEE EFFECTS

Yongli Cai⋆

Department of Mathematics, Sun Yat-Sen University
Guangzhou 510275, China
⋆ Corresponding author

Malay Banerjee

Department of Mathematics and Statistics, Indian Institute of Technology Kanpur
Kanpur, Uttar Pradesh, India

Yun Kang

Science and Mathematics Faculty, School of Letters and Sciences
Arizona State University, Mesa, AZ 85212, USA

Weiming Wang*

College of Mathematics and Information Science, Wenzhou University
Wenzhou, 325035 China
* Corresponding author

(Communicated by Haiyan Wang)

Abstract. In this article, we study the rich dynamics of a diffusive predator-prey system with Allee effects in the prey growth. Our model assumes a prey-dependent Holling type-II functional response and a density dependent death rate for predator. We investigate the dissipation and persistence property, the stability of nonnegative and positive constant steady state of the model, as well as the existence of Hopf bifurcation at the positive constant solution. In addition, we provide results on the existence and non-existence of positive non-constant solutions of the model. We also demonstrate the Turing instability under some conditions, and find that our model exhibits a diffusion-controlled formation growth of spots, stripes, and holes pattern replication via numerical simulations. One of the most interesting findings is that Turing instability in the model is induced by the density dependent death rate in predator.

1. Introduction.

Interaction between prey and predator has been a center research theme in ecology over many decades [1, 2, 5, 9, 15, 19, 24, 27, 33, 35, 39, 41, 54, 62, 65, 80, 81]. A wide variety of temporal prey-predator models have been investigated to help us understand the steady-state or oscillatory coexistence of both the species as well as the factors responsible for the system collapse through

---

2010 *Mathematics Subject Classification.* Primary: 35B36, 45M10; Secondary: 92C15.

Key words and phrases. Allee effects, density dependent, non-constant solution, turing instability, pattern formation.

The authors would like to thank Prof.Shangbin Cui in Sun Yat-Sen University and the anonymous referees for very helpful suggestions and comments which led to improvement of our original manuscript. This research was supported by the National Science Foundation of China (11171357 & 61373005). The research of Y. Kang was partially supported by Simons Collaboration Grants for Mathematicians (208902) and the research scholarship from School of Letters and Sciences.

the extinction of one or both the species. Prey-dependent functional responses play an important role in dynamics of prey-predator models. Gause type predator-prey models have been studied by many researchers [10, 26, 30, 31, 34, 36, 37, 38, 40, 44, 48, 49, 50, 63]. Gause type predator-prey models with logistic growth for prey and prey-dependent monotonic functional response can predict two types of dynamical scenario: stable coexistence and oscillatory coexistence [69]. The Gause type predator-prey models with non-monotonic prey-dependent functional response and/or predator's density dependent functional response exhibit very rich dynamic behavior [30, 31, 38].

Despite the complicated dynamics of temporal prey-predator models, these models may not be able to capture the dynamics observed in nature due to their homogeneous distribution assumption [55]. The spatiotemporal models of predator–prey interaction have been studied by many researchers, during the last four to five decades, to understand the role of random mobility of the individuals or organisms on the stability and persistence of interacting species [8, 11, 12, 13, 14, 21, 22, 43, 45, 46, 53, 56, 59, 61, 68, 71, 72, 77, 78].

Earlier works with the spatiotemporal models were based upon the derivation of Turing instability condition and determine the distribution of species over their habitats with the help of relevant numerical simulations [8, 13, 53, 77]. Considerable amount of attention has been paid to derive the analytical conditions for the existence and non-existence of non-constant positive steady-states for several reaction-diffusion equation models for prey-predator interactions. These investigations include the analysis of the predator-prey models with prey-dependent and predator-dependent functional responses [16, 56, 57, 58, 59, 60, 74, 75, 76]. Qualitative theories of the partial differential equations are used to obtain such results for the coupled nonlinear parabolic type partial differential equations.

Recently, significant amount of attention has been paid by the researchers to analyze the dynamic models of predator-prey interactions with Allee effect in the per capita prey growth rate [3, 4, 7, 25, 67, 66, 72, 82]. The so-called Allee effect in prey growth is described by the positive relationship between any component of individual fitness and either numbers or density of conspecifics [25, 67]. Generally speaking, a population is said to have an Allee effect, if it is initially an increasing function at low population density, then decreases to zero at higher prey density [72]. If the growth rate function is negative for a range of low prey density then the Allee effect is known as strong Allee effect and in case the prey growth rate function remain positive until the prey density reaches the carrying capacity is known as a weak Allee effect.

Gause type predator–prey models with Allee effect in prey growth, both strong and weak, and with prey-dependent as well as predator-dependent functional response has been investigated by the several researchers and various types of dynamic behaviors are reported [17, 18, 21, 42, 51, 52]. For example, Cai *et al* [21] considered a spatial prey-predator model with strong Allee effect in prey growth and Holling type II functional response. The authors have derived the conditions for nonexistence of nonconstant positive steady-state solution and instability conditions for the homogeneous as well as heterogeneous steady-states. Analytical findings reveal that the inclusion of Allee effect enhance the dynamic complexity of the spatio-temporal model. The mathematical techniques used in [21] to derive the analytical results are based upon the resources available in Refs.[6, 22, 23, 64].

In this paper, we focus on the spatiotemporal dynamics of a predator-prey model with (i) Allee effects in prey, (ii) prey-dependent Holling type-II functional response, and (iii) density dependent death rate for the predator. We aim to answer the following questions through our analytic and numerical results:

1. What is the effect of density dependent death rate for the predator on the spatiotemporal dynamics of our model?
2. How many stationary Turing patterns may there be in our model?

The rest of this article is organized as follows: In Section 2, we describe a predator–prey model with weak Allee effect in the prey growth and density dependent death rate for the predator. In Section 3, we study the large time behavior of time dependent solutions, that is to say, we investigate the dissipation and persistence property, the local and global stability of the nonnegative steady states of the model, as well as the existence of periodic solutions at the positive constant solution. In Section 4, we first give a prior estimates for the positive solutions of the model, then give some results on the existence and non-existence of positive nonconstant solutions of the model. In Section 5, we give the conditions of the Turing instability and perform a series of numerical simulation to show the occurrence of different patterns. The paper ends with a brief discussion in Section 6.

2. **Model derivation.**

Suppose that the prey individuals N and predator individuals P move randomly in the space, in this paper, we focus on the following prey-predator model with density dependent death rate for the predator:

$$\begin{cases} \dfrac{\partial N}{\partial t} = Ng(N) - \dfrac{cN}{N+a}P + d_1\Delta N, & x\in\Omega, t>0,\\ \dfrac{\partial P}{\partial t} = sP\left(-q-\delta P+\dfrac{cN}{N+a}\right) + d_2\Delta P, & x\in\Omega, t>0,\\ \dfrac{\partial N}{\partial \nu} = \dfrac{\partial P}{\partial \nu} = 0, & x\in\partial\Omega, t>0,\\ N(x,0)=N_0(x)\ge 0,\ P(x,0)=P_0(x)\ge 0, & x\in\Omega, \end{cases} \tag{1}$$

where $N(x,t), P(x,t)$ represent population densities of prey and predator at time t and location $x\in\Omega\subset\mathbb{R}^2$, respectively. Ω is a bounded domain with smooth boundary $\partial\Omega$. The function $\frac{cN}{N+a}$ describes the predator functional response, which is Holling type II functional response. c is the rate of capture and a is half saturation constant, q is the death rate of the predator and s is the feed concentration. The parameter δ is proportional to the density dependent death rate. The nonnegative constants d_1 and d_2 are the diffusion coefficients of $N(x,t)$ and $P(x,t)$, respectively. Δ is the Laplacian operator in two-dimensional space, which describes the random moving. ν is the outward unit normal vector of the boundary $\partial\Omega$. The main reason for choosing such boundary conditions is that we are interested in the self-organization of pattern, and the zero-flux boundary conditions imply that no external input is imposed from exterior [53].

In this paper, we consider the per capita growth function $g(N)$ as follows:

$$g(N) = r\Big(1-\frac{N}{K}\Big) - \frac{m}{N+b}, \tag{2}$$

where $\dfrac{m}{N+b}$ is the Allee effects term. And the positive parameters m and b are Allee effect constants, b is the population size at which fitness is half its maximum value. The constant m will allow the severity of the Allee effect to be modelled. r

is the intrinsic growth rate or biotic potential of the prey N, and K is the carrying capacity.

Notice that

$$\frac{dg(N)}{dN} = -\frac{r}{K} + \frac{m}{(N+b)^2} \quad \text{and} \quad \frac{d^2g(N)}{dN^2} = -\frac{2m}{(N+b)^3} < 0,$$

thus $g(N)$ is concave and has a unique critical point $N_c = \sqrt{mK/r} - b$. If where $g(N)$ is without predator, the temporal population dynamics of prey can be described by the following ODE:

$$\frac{dN}{dt} = Ng(N) = N\left(r\left(1 - \frac{N}{K}\right) - \frac{m}{N+b}\right), \tag{3}$$

whose dynamics can be summarized as follows:

1. **Allee effects:** If $N_c > 0$ (i.e., $m > \frac{b^2 r}{K}$), then $g(N)$ is increasing on $[0, N_c]$ and is decreasing on $[N_c, \infty)$. This is the case that we define prey has *Allee effects*, i.e., the per capita growth rate has positive correlation with population size at low population densities.
2. **Weak Allee effects:** If $\frac{b^2 r}{K} < m < br$, then prey has *weak Allee effects*. For any positive population, the prey population (3) approaches to
$$N_1 = \frac{r(K-b) + \sqrt{r^2(K-b)^2 + 4rK(br-m)}}{2r}.$$
3. **Strong Allee effects:** If $\frac{b^2 r}{K} < br < m < \frac{r^2(K-b)^2 + 4br^2K}{4rK}$, then prey has *strong Allee effects* with its *Allee threshold* defined as N_θ where
$$N_\theta = \frac{r(K-b) - \sqrt{r^2(K-b)^2 + 4rK(br-m)}}{2r}.$$
For any initial population in $[0, N_\theta)$, the prey population (3) goes to extinction; and for any initial population in (N_θ, ∞), the prey population (3) approaches to N_θ.

The main aim of this article is to investigate the spatiotemporal dynamics of model (1) in the case of weak Allee effect, i.e., $\frac{b^2 r}{K} < m < br$. The steady states of model (1) can be written as the following system of coupled elliptic equations:

$$\begin{cases} -d_1 \Delta N = N\left(r\left(1 - \frac{N}{K}\right) - \frac{m}{N+b}\right) - \frac{cN}{N+a}P, & x \in \Omega, \\ -d_2 \Delta P = sP\left(-q - \delta P + \frac{cN}{N+a}\right), & x \in \Omega, \\ \frac{\partial N}{\partial \nu} = \frac{\partial P}{\partial \nu} = 0, & x \in \partial\Omega. \end{cases} \tag{4}$$

In the next section, we study the large time behavior of time-dependent solutions. Especially, we focus on the global attractor and persistence property for solutions of model (1). Moreover, we investigate the stability of non-negative constant solutions of (1) and the existence of the Hopf bifurcation.

3. Large time behavior of time-dependent solutions.

To understand the large time behavior of model (1), our first task is to find the global attractor and the permanent conditions for the solutions.

3.1. **Global attractor and permanence.** In this subsection, we will focus on the global attractor and permanence of model (1). Firstly, we give an assumption.

Assumption 1. $q < c - \dfrac{ac}{a+K}$.

Lemma 3.1. *(Dissipation) Under Assumption 1, the non–negative solution* $(N(x, t), P(x,t))$ *of model (1) satisfies*

$$\limsup_{t\to\infty} \max_{\bar\Omega} N(x,t) \le K, \qquad \limsup_{t\to\infty} \max_{\bar\Omega} P(x,t) \le \frac{(c-q)K - aq}{\delta(a+K)}.$$

Proof. Since $N\left(r\left(1-\dfrac{N}{K}\right) - \dfrac{m}{N+b}\right) - \dfrac{cNP}{N+a} \le rN\left(1-\dfrac{N}{K}\right)$ in $\Omega\times[0,\infty)$, the first result follows easily from the simple comparison argument for parabolic problems [79], and thus there exists $T\in(0,\infty)$ such that $N(x,t)\le K+\varepsilon$ for $(x,t)\in\Omega\times[T,\infty)$ for an arbitrary constant $\varepsilon>0$. It then follows that $P(x, t)$ is a lower solution of the following problem

$$\begin{cases} \dfrac{\partial z}{\partial t} - d_2\Delta z = sz\left(-q-\delta z + \dfrac{c(K+\varepsilon)}{a+K+\varepsilon}\right), & x\in\Omega,\, t>T, \\ \dfrac{\partial z}{\partial \nu} = 0, & x\in\partial\Omega,\, t>T, \\ z(x,T) = P(x,\, T) > 0, & x\in\Omega. \end{cases} \tag{5}$$

The comparison argument [79] shows that

$$\limsup_{t\to\infty} \max_{\bar\Omega} P(x,t) \le \frac{(c-q)K - aq + (c-q)\varepsilon}{\delta(a+K+\varepsilon)}$$

which implies the second assertion for any $\varepsilon>0$ sufficiently small. □

Remark 1. Lemma 3.1 shows that

$$\mathbf{\Gamma} := [0,K]\times\left[0, \frac{(c-q)K-aq}{\delta(a+K)}\right] \tag{6}$$

is a global attractor for all solutions of model (1) in the sense that any non–negative solution $(N(x,t),P(x,t))$ of model (1) enters in $\mathbf{\Gamma}$ for large t and for all $x\in\Omega$.

The following lemma gives sufficient conditions for the permanence of the solutions for model (1).

Lemma 3.2. *Under Assumption 1, if condition*

$$m < br\left(1 - \frac{c((c-q)K-aq)}{ar\delta(a+K)} - \frac{aq}{K(c-q)}\right) \tag{7}$$

holds, then any positive solution $(N(x,t),P(x,t))$ *of (1) satisfies*

$$\liminf_{t\to\infty} \min_{\bar\Omega} N(x,\, t) \ge \alpha, \quad \liminf_{t\to\infty} \min_{\bar\Omega} P(x,\, t) \ge \frac{(c-q)\alpha - aq}{a+\alpha}.$$

where $\alpha = \dfrac{K}{r}\left(r - \dfrac{m}{b} - \dfrac{c((c-q)K-aq)}{a\delta(a+K)}\right)$.

Proof. In view of Lemma 3.1, there exists a $T\in(0,\infty)$ such that

$$P(x,t) \le \frac{(c-q)K-aq}{\delta(a+K)} + \frac{a\varepsilon}{c}$$

in $\Omega \times [T, \infty)$ for an arbitrary $\varepsilon > 0$. Thus we have that $N(x,t)$ is an upper solution of

$$\begin{cases} \dfrac{\partial z}{\partial t} - d_1 \Delta z = z\left(r - \dfrac{m}{b} - \dfrac{c((c-q)K - aq)}{a\delta(a+K)} - \varepsilon - \dfrac{r}{K}N\right), & x \in \Omega,\ t > T, \\ \dfrac{\partial z}{\partial \nu} = 0, & x \in \partial\Omega,\ t > T, \\ z(x,T) = N(x,\, T) > 0, & x \in \Omega. \end{cases} \tag{8}$$

Let $N(t)$ be the unique positive solution of the following problem

$$\begin{cases} \dot{w} = w\left(r - \dfrac{m}{b} - \dfrac{c((c-q)K - aq)}{a\delta(a+K)} - \varepsilon - \dfrac{r}{K}w\right), & t > T, \\ w(T) = \min\limits_{\bar{\Omega}} N(x, T) > 0. \end{cases}$$

Then $N(t)$ is a lower solution of model (8). It follows from (7) that

$$m < b\left(r - \frac{c((c-q)K - aq)}{a\delta(a+K)}\right) = b\tau(0) \quad \text{where} \quad \tau(\varepsilon) = r - \frac{c((c-q)K - aq)}{a\delta(a+K)} - \varepsilon,$$

thus there exists a sufficiently small $\varepsilon > 0$ such that $m < b\tau(\varepsilon)$. So that we have $r - \dfrac{m}{b} - \dfrac{c((c-q)K - aq)}{a\delta(a+K)} - \varepsilon > 0$. Due to the arbitrariness of ε, we find

$$\lim_{t\to\infty} N(t) = \frac{K}{r}\left(r - \frac{m}{b} - \frac{c((c-q)K - aq)}{a\delta(a+K)}\right) := \alpha.$$

An application of the comparison principle [79] gives the desired limit for $N(x,t)$. Now one can find $T_0 \geq T$ such that $N(x,t) \geq \alpha - \varepsilon$ in $[T_0, \infty) \times \Omega$ for a sufficiently small but arbitrary $\varepsilon > 0$, and thus $P(x,t)$ is an upper solution of

$$\begin{cases} \dfrac{\partial z}{\partial t} - d_2 \Delta z = sz\left(-q - \delta z + \dfrac{c(\alpha - \varepsilon)}{a + \alpha - \varepsilon}\right), & x \in \Omega,\ t > T_0, \\ \dfrac{\partial z}{\partial \nu} = 0, & x \in \partial\Omega,\ t > T_0, \\ z(x, T_0) = P(x,\, T_0) > 0, & x \in \Omega. \end{cases} \tag{9}$$

Let us define,

$$\rho(\varepsilon) = \frac{K}{r}\left(r - \frac{m}{b} - \frac{c((c-q)K - aq)}{a\delta(a+K)}\right)(c-q) - aq + (q-c)\varepsilon$$

then it is easy to check that $\rho(0) > 0$ by the assumption mentioned in (7). Since $\rho(\varepsilon)$ is decreasing in ε under *Assumption 1* and $\lim\limits_{\varepsilon\to\infty} \rho(\varepsilon) = -\infty$, there exists a unique $\tilde{\varepsilon}$ such that $\rho(\tilde{\varepsilon}) = 0$. By choosing a sufficiently small $\varepsilon > 0$ with $\varepsilon < \tilde{\varepsilon}$, we have $\rho(\varepsilon) > 0$, and thus using the comparison argument [79] we find,

$$\liminf_{t\to\infty} \min_{\bar{\Omega}} P(x,\, t) \geq \frac{(c-q)\alpha - aq}{a + \alpha},$$

and hence the proof. $\square$

A direct application of Lemma 3.1 and Lemma 3.2 gives the following theorem.

Theorem 3.3. *(Permanence) If Assumption 1 and condition (7) hold, there exist constants* $0 < \epsilon < C < \infty$ *such that*

$$\epsilon < \liminf_{t\to\infty} \min_{\bar{\Omega}} N(x,\,t) < \limsup_{t\to\infty} \max_{\bar{\Omega}} N(x,\,t) < C,$$
$$\epsilon < \liminf_{t\to\infty} \min_{\bar{\Omega}} P(x,\,t) < \limsup_{t\to\infty} \max_{\bar{\Omega}} P(x,\,t) < C.$$

That is, model (1) is permanent.

3.2. **Stability of non-negative constant steady states.** In this subsection, we discuss the stability of various constant steady states. The concerned steady-states are also known as homogeneous steady-states.

3.2.1. *Existence of non-negative constant steady state solutions.* Apart from the trivial constant steady state $E_0 = (0,0)$, the other non–negative constant steady states of model (1) are the non-negative solutions of the following two coupled equations,

$$\begin{cases} P = \dfrac{1}{c}(N+a)\left(r\left(1-\frac{N}{K}\right)-\frac{m}{N+b}\right) = \dfrac{1}{c}(N+a)g(N) := h_1(N), \\ P = \dfrac{1}{\delta(N+a)}\big((c-q)N-aq\big) := h_2(N). \end{cases} \tag{10}$$

For $P=0$, from $h_1(N)=0$, we can get one semi–trivial constant steady state

$$N_1 = \frac{r(K-b)+\sqrt{r^2(K-b)^2-4rK(m-br)}}{2r},$$

and there is no constant steady state with $N=0$.

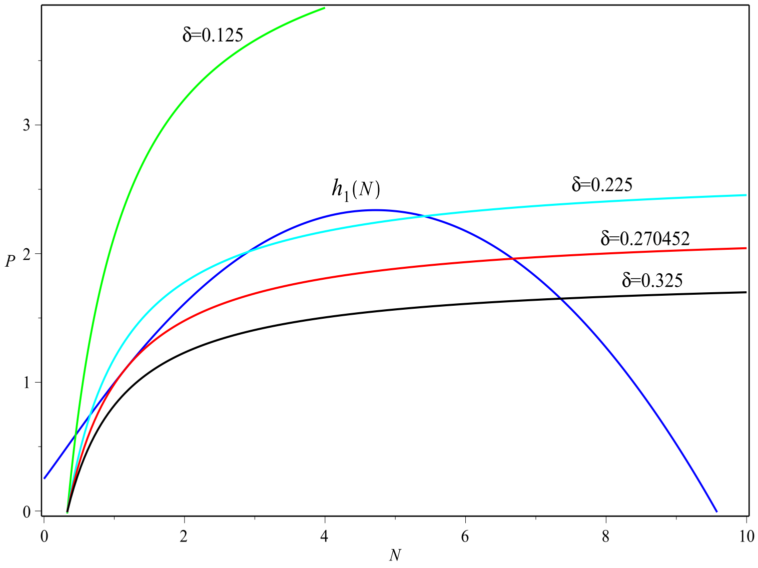

Figure 1. The positive constant solutions of model (1). Blue curve is the prey nullcline and predator nullclines are depicted in green ($\delta = 0.125$, one), cyan ($\delta = 0.225$, three), red ($\delta = 0.270452$, two) and black ($\delta = 0.325$, one) color. The blue line is based on $h_1(N)$, and others $h_2(N)$.

For the existence of positive constant solution, after solving N from the second equation $h_2(N) = P$ and substituting it into the first equation $h_1(N) = P$, we can obtain a polynomial equation about P with degree 5, therefore the equation at least has one real root. That is to say, model (1) may be having one or more positive equilibria, namely $E^* = (N^*, P^*)$.

In Fig.1, as an example, four plots of the predator nullcline is presented for four different values of δ and keeping other parameters fixed at $r = 1$, $K = 10$, $m = 0.45$, $b = 0.9$, $c = 1$, $a = 0.5$ and $q = 0.4$. When $\delta = 0.125$, model (1) has one positive constant steady state; and $\delta = 0.225$, there are three positive constant steady states; $\delta = 0.270452$, model (1) has two positive constant steady states; while $\delta = 0.325$, model (1) has one positive constant steady state. In addition, note that the plots of $h_1(N)$ is a parabola with downward opening, thus we can know that model (1) at least has one positive constant steady state. From Fig.1, one can know that the number of interior constant steady states varies from 1 to 3 depending upon the magnitude of δ.

Remark 2. If there is no density dependent death rate for the predator, i.e. $\delta = 0$, the existence of non-negative constant steady state solutions of model (1) can be seen in [21] in details.

3.2.2. *Local stability of non-negative constant steady states.* In this subsection, we shall analyze the locally asymptotic stability of the non–negative constant steady states for model (1).

For the sake of simplicity, we rewrite model (1) in a compact form as follows:

$$\begin{cases} \mathbf{w}_t = D\Delta \mathbf{w} + F(\mathbf{w}), & x \in \Omega, t > 0, \\ \dfrac{\partial \mathbf{w}}{\partial \nu} = 0, & x \in \partial\Omega,\ t > 0, \\ \mathbf{w}(x,0) = (N_0(x), P_0(x)^T, & x \in \Omega, \end{cases} \tag{11}$$

where $\mathbf{w} = (N(x,t),\ P(x,t))^T$, $D = \operatorname{diag}(d_1,\ d_2)$ and

$$F(\mathbf{w}) = \begin{pmatrix} N\left(r\left(1 - \dfrac{N}{K}\right) - \dfrac{m}{N+b} - \dfrac{cP}{N+a}\right) \\ sP\left(-q - \delta P + \dfrac{cN}{N+a}\right) \end{pmatrix}.$$

Let $0 = \mu_0 < \mu_1 < \mu_2 < \cdots$ be the eigenvalues of the operator $-\Delta$ on Ω with the zero–flux boundary conditions, and $E(\mu_i)$ be the eigenspace corresponding to μ_i in $H^1(\bar{\Omega})$. Let

$$\mathbf{X} = \left\{ \mathbf{w} \in [H^1(\Omega)]^2 \,\middle|\, \partial_\nu \mathbf{w} = 0 \text{ on } \partial\Omega \right\}, \tag{12}$$

$\left\{\phi_{ij} | j = 1, ..., \dim E(\mu_i)\right\}$ be an orthonormal basis of $E(\mu_i)$, $\mathbf{X}_{ij} = \left\{ \mathbf{c}\phi_{ij} \middle| \mathbf{c} \in \mathbb{R}^2 \right\}$, then

$$\mathbf{X} = \bigoplus_{i=1}^{\infty} \mathbf{X}_i, \quad \text{where} \quad \mathbf{X}_i = \bigoplus_{j=1}^{\dim E(\mu_i)} \mathbf{X}_{ij} \tag{13}$$

Next, we give the main results on the local stability of the non–negative constant steady states of model (1). For the proof of this, we need the following assumption.

Assumption 2.
(a) $g(N^*) + (N^* + a)g'(N^*) > 0$;
(b) $\delta(a + N^*)^2)((a + N^*)g'(N^*) + g(N^*)) - ac^2 < 0$,
where $g'(N^*) = \frac{m}{(N^* + b)^2} - \frac{r}{K}$.

Theorem 3.4. *(a) For the positive constant steady state* $E^* = (N^*, P^*)$ *of model (1):*
(a1) under Assumptions 2, it is locally asymptotically stable if

$$s > \max\left\{\frac{d_2 c N^*(g(N^*) + (a + N^*)g'(N^*))}{d_1 \delta (a + N^*)^2 g(N^*)}, \frac{cN^*(g(N^*) + (a + N^*)g'(N^*))}{\delta (a + N^*)^2 g(N^*)}\right\}. \tag{14}$$

(a2) If $g(N^*) + (N^* + a)g'(N^*) < 0$*, it is locally asymptotically stable.*

(b) The semi–trivial constant steady state $E_1 = (N_1, 0)$ *of model (1) is locally asymptotically stable if* $\frac{r(K - b) + \sqrt{r^2(K - b)^2 - 4rK(m - br)}}{2r} < \frac{aq}{c - q}$.

Proof. (a) The linearization of model (1) at the positive constant steady state $E^* = (N^*, P^*)$ can be expressed by:

$$\mathbf{w}_t = \pounds(\mathbf{w}) \equiv D\Delta\mathbf{w} + J\mathbf{w},$$

where

$$J = \begin{pmatrix} N^* g'(N^*) + \frac{cN^*P^*}{(a + N^*)^2} & -\frac{cN^*}{a + N^*} \\ \frac{acsP^*}{(a + N^*)^2} & -s\delta P^* \end{pmatrix}.$$

For each $i \geq 0$, $\mathbf{X}_i$ is invariant under the operator $\pounds$, and λ is an eigenvalue of $\pounds$ if and only if λ is an eigenvalue of the matrix $A_i = -\mu_i D + J$ for some $i \geq 0$. Thus the stability of the positive constant steady state is reduced to consider the characteristic equation $\mathrm{Det}(\lambda I - A_i) = 0$, where,

$$\det(\lambda I - A_i) = \lambda^2 - \mathrm{Tr}(A_i)\lambda + \mathrm{Det}(A_i) := \varphi_i(\lambda), \tag{15}$$

and

$$\mathrm{Tr}(A_i) = -\mu_i(d_1 + d_2) + \mathrm{Tr}(J),$$

$$\mathrm{Det}(A_i) = d_1 d_2 \mu_i^2 - \left(d_2 N^* \left(g'(N^*) + \frac{g(N^*)}{a + N^*}\right) - d_1 s\delta P^*\right)\mu_i + \mathrm{Det}(J),$$

with

$$\mathrm{Tr}(J) = N^* \left(g'(N^*) + \frac{g(N^*)}{a + N^*}\right) - s\delta P^*,$$

$$\mathrm{Det}(J) = -\frac{sN^*P^*}{(a + N^*)^3}\Big(\delta(a + N^*)^2)((a + N^*)g'(N^*) + g(N^*)) - ac^2\Big).$$

If $g(N^*) + (N^* + a)g'(N^*) < 0$, we have $\mathrm{Tr}(A_i) < 0$, $\mathrm{Det}(A_i) > 0$. If *Assumptions* 2 and (14), one can check that $\mathrm{Tr}(J) < 0$, $\mathrm{Det}(J) > 0$. It follows from (14) that $\mathrm{Det}(A_i) > 0 > \mathrm{Tr}(A_i)$ for $i \geq 0$. Therefore, the eigenvalues of the matrix $-\mu_i D + J$ have negative real parts. It thus follows from the Routh–Hurwitz criterion that, for each $i \geq 0$, the two roots λ_{i1} and λ_{i2} of $\varphi_i(\lambda) = 0$ all have negative real parts.

In the following, we prove that there exists an $\eta > 0$ such that

$$\mathrm{Re}\{\lambda_{i1}\} \leq -\eta, \quad \mathrm{Re}\{\lambda_{i2}\} \leq -\eta. \tag{16}$$

Let $\lambda = \mu_i \xi$, then

$$\varphi_i(\lambda) = \mu_i^2 \xi^2 - \mathrm{Tr}(A_i)\mu_i \xi + \mathrm{Det}(A_i) := \tilde{\varphi}_i(\xi). \tag{17}$$

Since $\mu_i \to \infty$ as $i \to \infty$, it follows that

$$\lim_{i\to\infty} \frac{\tilde{\varphi}_i(\xi)}{\mu_i^2} = \xi^2 + (d_1 + d_2)\xi + d_1 d_2 := \tilde{\varphi}(\xi). \tag{18}$$

Clearly, $\tilde{\varphi}(\xi)$ has two negative roots: $-d_1$ and $-d_2$. Thus, let $\tilde{d} = \min\{d_1, d_2\}$, then $\mathrm{Re}\{\xi_1\}, \mathrm{Re}\{\xi_2\} \leq -\tilde{d}$. By continuity, we see that there exists i_0 such that the two roots ξ_{i1}, ξ_{i2} of $\tilde{\varphi}_i(\xi) = 0$ satisfy $\mathrm{Re}\{\xi_{i1}\} \leq -\frac{\tilde{d}}{2}, \mathrm{Re}\{\xi_{i2}\} \leq -\frac{\tilde{d}}{2}$, $\forall i \geq i_0$. In turn, $\mathrm{Re}\{\lambda_{i1}\}, \mathrm{Re}\{\lambda_{i2}\} \leq -\frac{\mu_i \tilde{d}}{2} \leq -\frac{\tilde{d}}{2}$, $\forall i \geq i_0$. Let

$$-\tilde{\eta} = \max_{1\leq i\leq i_0} \Big\{\mathrm{Re}\{\lambda_{i1}\}, \mathrm{Re}\{\lambda_{i2}\}\Big\}.$$

Then $\tilde{\eta} > 0$ and (16) holds for $\eta = \min\left\{\tilde{\eta}, \dfrac{\tilde{d}}{2}\right\}$.

Consequently, the spectrum of $\pounds$, which consists of eigenvalues, lies in $\{\mathrm{Re}\lambda \leq -\eta\}$. In the sense of [32], we obtain that the positive constant steady state solution $E^* = (N^*,\, P^*)$ of the model (1) is uniformly asymptotically stable.

(b) The linearization of model (1) at the semi–trivial constant steady state $E_1 = (N_1,\, 0)$ can be expressed by:

$$\mathbf{w}_t = \pounds(\mathbf{w}) = D\Delta\mathbf{w} + J_1\mathbf{w},$$

where

$$J_1 = \begin{pmatrix} N_1\left(\dfrac{m}{(N_1+b)^2} - \dfrac{r}{K}\right) & -\dfrac{cN_1}{a+N_1} \\ 0 & s\left(-q + \dfrac{cN_1}{a+N_1}\right) \end{pmatrix},$$

It follows from $\dfrac{r(K-b) + \sqrt{r^2(K-b)^2 - 4rK(m-br)}}{2r} < \dfrac{aq}{c-q}$ that $\mathrm{Tr}(J_1) < 0$, $\mathrm{Det}(J_1) > 0$. The remaining arguments are rather similar as above. The proof is complete. □

3.2.3. *Global stability of positive constant steady states.* In this subsubsection, we explore sufficient conditions of global stability of the positive constant steady state solution $E^* = (N^*,\, P^*)$ for model (1) with weak Allee effect (i.e. $\frac{b^2 r}{K} < m < br$). Before stating the main theorem, we recall the following result which can be found in [73].

Lemma 3.5. [73] *Let c_1 and c_2 be two positive constants. Assume that $\varphi, \psi \in C^1([c_1, \infty))$, $\psi(t) \geq 0$ and φ is bounded from below. If $\varphi'(t) \leq -c_2\psi(t)$ and $\psi'(t) \leq c_3$ in $[c_1, \infty)$ for some constant c_3, then $\lim_{t\to\infty} \psi(t) = 0$.*

In the following, C denotes a generic positive constant which does not depend on $x \in \bar{\Omega}$ and $t \geq 0$.

Theorem 3.6. *Under Assumptions 1 and 2, the positive constant steady state solution $E^* = (N^*,\, P^*)$ of model (1) is globally asymptotically stable if the following* *condition holds:*

$$\frac{m}{b(N^*+b)}+\frac{g(N^*)}{a}<\frac{r}{K}. \tag{19}$$

Proof. By Lemma 3.1, the solution $(N(x,t),P(x,t))$ of model (1) is bounded uniformly on $\bar{\Omega}$, that is, $\|N(\cdot,t)\|_\infty,\|P(\cdot,t)\|_\infty\le C$. Furthermore, it follows from Theorem A_2 in [20] that

$$\|N(\cdot,t)\|_{C^{2+\alpha}(\bar{\Omega})},\|P(\cdot,t)\|_{C^{2+\alpha}(\bar{\Omega})}\le C,\quad \forall\, t\ge 1,\alpha\in(0,1). \tag{20}$$

We adopt the Lyapunov function:

$$V(t)=\int\limits_\Omega\Big[V_1(N(x,\,t))+V_2(P(x,\,t))\Big]dx, \tag{21}$$

where $V_1(N)=\int_{N^*}^{N}\frac{\xi-N^*}{\xi}d\xi$, $V_2(P)=\frac{(N^*+a)}{as}\int_{P^*}^{P}\frac{\eta-P^*}{\eta}d\eta$. Then $V(t)\ge 0$ and $V(t)=0$ if and only if $(N,P)=(N^*,P^*)$. Then,

$$\begin{aligned}\frac{dV}{dt}&=\int\limits_\Omega\left(\frac{(N-N^*)}{N}\frac{\partial N}{\partial t}+\frac{(N^*+a)}{as}\frac{(P-P^*)}{P}\frac{\partial P}{\partial t}\right)dx\\&=\int\limits_\Omega(N-N^*)\left(r-\frac{rN}{K}-\frac{m}{N+b}-\frac{cP}{N+a}+d_1\frac{\Delta N}{N}\right)dx\\&\quad+\frac{N^*+a}{a}\int\limits_\Omega(P-P^*)\left(-q-\delta P+\frac{cN}{N+a}+d_2\frac{\Delta P}{sP}\right)dx\\&=\int\limits_\Omega I(N,\,P)dx-d_1N^*\int\limits_\Omega\frac{|\nabla N|^2}{N^2}dx-\frac{d_2(N^*+a)P^*}{as}\int\limits_\Omega\frac{|\nabla P|^2}{P^2}dx,\end{aligned}$$

where

$$\begin{aligned}I(N,\,P)\quad&=(N-N^*)\left(r-\frac{rN}{K}-\frac{m}{N+b}-\frac{cP}{N+a}\right)\\&\quad+\frac{N^*+a}{a}(P-P^*)\left(-q-\delta P+\frac{cN}{N+a}\right).\end{aligned}$$

After some algebraic calculations, we have

$$\begin{aligned}&I(N,\,P)\\&=-(N-N^*)^2\left(\frac{r}{K}-\frac{m}{(N^*+b)(N+b)}-\frac{cP^*}{(N^*+a)(N+a)}\right)\\&\quad-\frac{\delta(N^*+a)}{a}(P-P^*)^2\\&\le-(N-N^*)^2\left(\frac{r}{K}-\frac{m}{b(N^*+b)}-\frac{cP^*}{a(N^*+a)}\right)-\frac{\delta(N^*+a)}{a}(P-P^*)^2.\end{aligned} \tag{22}$$

In view of (19), we have

$$I(N,\,P)\le -C\Big((N-N^*)^2+(P-P^*)^2\Big).$$

It follows from (20) that

$$\frac{dV}{dt}\le -C\left(\int\limits_\Omega\Big((N-N^*)^2+(P-P^*)^2+|\nabla N|^2+|\nabla P|^2\Big)dx\right),$$

and

$$\begin{aligned}&\frac{d}{dt}\left(\int\limits_{\Omega}\Big((N-N^*)^2+(P-P^*)^2+|\nabla N|^2+|\nabla P|^2\Big)dx\right)\\&=2\int\limits_{\Omega}(N_t(N-N^*)+P_t(P-P^*)+N_t\Delta N+P_t\Delta P)\,dx\\&\leq C.\end{aligned}$$

Hence, by Lemma 3.5, we get

$$\lim_{t\to\infty}\int_{\Omega}(N-N^*)^2dx=0,\ \lim_{t\to\infty}\int_{\Omega}(P-P^*)^2dx=0,\ \lim_{t\to\infty}\int_{\Omega}(|\nabla N|^2+|\nabla P|^2)dx=0. \tag{23}$$

It follows from the Poincaré inequality that

$$\lim_{t\to\infty}\int_{\Omega}(N-\bar{N})^2dx=\lim_{t\to\infty}\int_{\Omega}(P-\bar{P})^2dx=0, \tag{24}$$

where $\bar{N}(t)=\dfrac{1}{|\Omega|}\displaystyle\int_{\Omega}Ndx$. Clearly,

$$|\Omega||\bar{N}(t)-N^*|^2=\int_{\Omega}(\bar{N}-N^*)^2dx\leq 2\int_{\Omega}(N-\bar{N})^2dx+2\int_{\Omega}(N-N^*)^2dx.$$

From (23) and (24), we have

$$\lim_{t\to\infty}\bar{N}(t)=N^*,\ \lim_{t\to\infty}\bar{P}(t)=P^*. \tag{25}$$

On the other hand, (20) implies that there exists a subsequence of $\{t_n\}$ and non–negative functions $\tilde{N},\tilde{P}\in C^2(\bar{\Omega})$ such that

$$\lim_{n\to\infty}(\|N(\cdot,t_n)-\tilde{N}\|_{C^2(\bar{\Omega}}, \|P(\cdot,t_n)-\tilde{P}\|_{C^2(\bar{\Omega})})=(0,0).$$

In view of (25), we know that $\tilde{N}=N^*,\tilde{P}=P^*$. Therefore,

$$\lim_{n\to\infty}(\|N(\cdot,t_n)-N^*\|_{C^2(\bar{\Omega}}, \|P(\cdot,t_n)-P^*\|_{C^2(\bar{\Omega})})=(0,0).$$

Thus, from this and the local asymptotic stability of E^* we can conclude that the homogeneous steady-state E^* is globally asymptotically stable. □

Remark 3. According to Theorem 3.6, the global stability of $E^*=(N^*,\ P^*)$ of model (1) with weak Allee effect means that, however quickly or slowly the two species diffuse, they will be spatially homogeneously distributed as time converges to infinity.

3.3. **Hopf bifurcation.**

In this subsection, we derive the conditions of Hopf bifurcation for model (1), that is the condition under which the coexisting homogeneous steady-state loses stability through Hopf-bifurcation.

For the emergency of the Hopf bifurcation at the positive constant steady state E^*, the matrix $A_i=-\mu_iD+J$ must have an eigenvalue on the imaginary axis [47], i.e. $\mathrm{Tr}(A_i)\equiv 0$. The only possible critical values of m are $m(k)$ such that

$$-\mu_k(d_1+d_2)+N^*\left(\frac{m(k)}{(N^*+b)^2}-\frac{r}{K}\right)+\frac{cN^*P^*}{(a+N^*)^2}-s\delta P^*=0,$$

for $k\geq 0$. At $m=m(k)$, $\mathrm{Tr}(A_i)=(d_1+d_2)(\mu_k-\mu_i)$, and therefore if $k\geq 1$, then $\mathrm{Tr}(A_i)>0$ for all $0\leq i<k$ and the matrix $A_i=-\mu_iD+J$ has at least $2k$

eigenvalues with positive real parts. Therefore, the only value of s at which Hopf bifurcation hypotheses may be satisfied is

$$s = s(0) := \frac{N^*}{\delta P^*}\left(\frac{cP^*}{(N^*+a)^2} + \frac{m}{(N^*+b)^2} - \frac{r}{K}\right). \tag{26}$$

Near $s(0)$, the complex conjugate pair $\kappa(s) \pm i\omega(s)$ is given by

$$\kappa(s) = \frac{1}{2}\mathrm{Tr}(J),\ \omega^2(s) = \mathrm{Det}(J) - \kappa^2(s).$$

since $\kappa(s(0) = 0$ and $\mathrm{Det}(J) > 0$, we have $\omega^2(s) \neq 0$. In addition, it is easy to check

$$\frac{d}{ds}\kappa(s)|_{s=s(0)} = -\delta P^* \neq 0,$$

and thus we have the following theorem.

Theorem 3.7. *(Hopf bifurcation) Under Assumption 2, then the constant steady-state E^* of model (1) loses stability through Hopf bifurcation at*

$$s = \frac{cN^*(g(N^*) + (a+N^*)g'(N^*))}{\delta(a+N^*)^2 g(N^*)}.$$

4. Non–constant time-independent positive steady states.

For model (1) or (4), the existence of a nonconstant time-independent positive solution, also called stationary pattern, is an indication of the richness of the corresponding partial differential equation dynamics. In recent years, stationary pattern induced by diffusion has been studied extensively, and many important phenomena have been observed [59].

In this section, we discuss the existence and non-existence of non–constant steady states of model (1).

4.1. A priori estimates for positive solutions of model (4).

From now on, we will deduce a *priori* estimates of positive upper and lower bounds for positive solutions of model (4). In order to obtain the desired bounds, we recall the following maximum principle [45] and Harnack Inequality [43]. For simplicity, denote $\Theta := (r, K, m, a, b, c, q, \delta, s)$.

Lemma 4.1. *(Maximum principle [45]) Let Ω be a bounded Lipschitz domain in $\mathbb{R}^n$ and $g \in C(\bar{\Omega} \times \mathbb{R})$.*

(a) Assume that $w \in C^2(\Omega) \cap C^1(\bar{\Omega})$ and satisfies

$$\Delta w(x) + g(x, w(x)) \geq 0 \quad in \quad \Omega, \qquad \frac{\partial w}{\partial \nu} \leq 0 \quad on \quad \partial\Omega.$$

If $w(x_M) = \max_{\bar{\Omega}} w(x)$, then $g(x_M, w(x_M)) \geq 0$.

(b) Assume that $w \in C^2(\Omega) \cap C^1(\bar{\Omega})$ and satisfies

$$\Delta w(x) + g(x, w(x)) \leq 0 \quad in \quad \Omega, \qquad \frac{\partial w}{\partial \nu} \geq 0 \quad on \quad \partial\Omega.$$

If $w(x_m) = \min_{\bar{\Omega}} w(x)$, then $g(x_m, w(x_m)) \leq 0$.

Lemma 4.2. *(Harnack Inequality [43]) Let $w \in C^2(\Omega) \cap C^1(\bar{\Omega})$ be a positive solution to $\Delta w(x) + c(x)w(x) = 0$, where $c \in C(\bar{\Omega})$, satisfying zero–flux boundary conditions on $\bar{\Omega}$. Then there exists a positive constant $C^* = C^*(\|c\|_\infty, \Omega)$, such that*

$$\max_{\bar{\Omega}} w \leq C^* \min_{\bar{\Omega}} w.$$

Now we state and prove the relevant theorem for the bounds of the solutions for the model (4) over its domain of definition Ω.

Theorem 4.3. *(The bounds of the solutions) Assume that Assumption 1 holds. Let* $\tilde{d}$ *be an arbitrary fixed positive number. There exists a positive constant* $C = C(\Gamma)$*, such that if* $d_1, d_2 \geq \tilde{d}$*, any positive solution* $(N(x), P(x))$ *of model (4) satisfies*

$$C \leq N(x), P(x) \leq \max\left\{K, \frac{(c-q)K - aq}{\delta(a+K)}\right\}. \tag{27}$$

Proof. In view of *Assumption 1*, by applying Lemma 3.1, it is easy to see that

$$N(x), P(x) \leq \max\left\{K, \frac{(c-q)K - aq}{\delta(a+K)}\right\}.$$

Let $c_1(x) = \dfrac{1}{d_1}\left(Ng(N) - \dfrac{cN}{N+a}P\right)$, $c_2(x) = \dfrac{1}{d_2}sP\left(-q - \delta P + \dfrac{cN}{N+a}\right)$. Then, in view of the second of inequality of (27), there exists a positive constant $C = C(\Gamma)$ such that $\|c_1(x)\|_\infty, \|c_2(x)\|_\infty \leq C$ provided that $d_1, d_2 > \tilde{d}$.

Now, it suffices to verify the lower bounds of $N(x)$ and $P(x)$. We will verify the conclusion by a contradiction argument.

On the contrary, suppose that the conclusion is not true, then, by Lemma 4.2, there exist sequences $\{d_{1,i}\}_{i=1}^{\infty}$ and $\{d_{2,i}\}_{i=1}^{\infty}$ with $d_{1,i},\ d_{2,i} > \tilde{d}$ and the positive solution (N_i, P_i) of model (4) corresponding to $(d_1, d_2) = (d_{1,i}, d_{2,i})$, such that

$$\max_{\overline{\Omega}} N_i(x) \to 0 \quad \text{or} \quad \max_{\overline{\Omega}} P_i(x) \to 0 \quad \text{as} \quad i \to \infty, \tag{28}$$

and $(N_i,\ P_i)$ satisfies

$$\begin{cases} -d_{1,i}\Delta N_i = N_i\left(r - \dfrac{r}{K}N_i - \dfrac{m}{N_i+b} - \dfrac{cP_i}{N_i+a}\right), & x \in \Omega, \\ -d_{2,i}\Delta P_i = sP_i\left(-q - \delta P_i + \dfrac{cN_i}{N_i+a}\right), & x \in \Omega, \\ \dfrac{\partial N_i}{\partial \nu} = \dfrac{\partial P_i}{\partial \nu} = 0, & x \in \partial\Omega. \end{cases}$$

Integrating by parts, we obtain that, for $i = 1, 2, ...,$

$$\begin{cases} \displaystyle\int_\Omega N_i\left(r - \frac{r}{K}N_i - \frac{m}{N_i+b} - \frac{cP_i}{N_i+a}\right)dx = 0, \\ \displaystyle\int_\Omega sP_i\left(-q - \delta P_i + \frac{cN_i}{N_i+a}\right)dx = 0. \end{cases} \tag{29}$$

By the regularity theory for elliptic equations [29], we see that there exists a subsequence of $\{(N_i, P_i)\}_i^\infty$ and two non–negative functions $\tilde{N}, \tilde{P} \in C^2(\Omega)$, such that $(N_i, P_i) \to (\tilde{N}, \tilde{P})$ in $[C^2(\Omega)]^2$ as $i \to \infty$. By (28), we have that $\tilde{N} \equiv 0$ or $\tilde{P} \equiv 0$.

Letting $i \to \infty$ in (29) we obtain that

$$\begin{cases} \displaystyle\int_\Omega \tilde{N}\left(r - \frac{r}{K}\tilde{N} - \frac{m}{\tilde{N}+b} - \frac{c\tilde{P}}{\tilde{N}+a}\right)dx = 0, \\ \displaystyle\int_\Omega s\tilde{P}\left(-q - \delta\tilde{P} + \frac{c\tilde{N}}{\tilde{N}+a}\right)dx = 0. \end{cases} \tag{30}$$

We consider the following two cases:

Case 1. $\tilde{N} \equiv 0$. The first equation of (29) shows that there exists $x_i \in \bar{\Omega}$ such that

$$r - \frac{r}{K} N_i(x_i) - \frac{m}{N_i(x_i) + b} - \frac{cP_i(x_i)}{N_i(x_i) + a} = 0.$$

Assume $x_i \to x_0 \in \bar{\Omega}$ as $i \to \infty$, it follows from $m < br$ that

$$\tilde{P}(x_0) = \frac{a}{c}\left(r - \frac{m}{b}\right) > 0, \tag{31}$$

and the second equation of (30) becomes $\int_\Omega s\tilde{P}(-q - \delta\tilde{P})dx = 0$, which implies $\tilde{P} \equiv 0$. This contradicts the result (31).

Case 2. $\tilde{P} \equiv 0$. The first equation of (30) becomes

$$\int_\Omega \tilde{N}\left(r - \frac{r}{K}\tilde{N} - \frac{m}{\tilde{N} + b}\right) dx = 0.$$

As $\frac{1}{2}\tilde{\varepsilon} \le N(x) \le K$, it follows that $\tilde{N} = \frac{r(K-b) + \sqrt{r^2(K-b)^2 + 4rK(br-m)}}{2r} = N_1$, and the second equation of (30) becomes

$$\int_\Omega s\tilde{P}\left(-q - \delta\tilde{P} + \frac{cN_1}{N_1 + a}\right) dx = 0.$$

Since $\frac{aq}{c-q} > N_1$, we have

$$\tilde{P} = \frac{1}{\delta}\Big((c-q)N_1 - aq\Big),$$

which derives a contradiction. This completes the proof. □

4.2. **Non–existence of non–constant positive steady states.** In Theorem 3.6, the global asymptotic stability of the positive constant steady state implies the non–existence of non–constant steady state of model (1) regardless of the diffusion coefficients. This subsection is devoted to the consideration of the non–existence for the non–constant positive solutions of model (4), and in the below results, the diffusion coefficients do play a significant role.

Theorem 4.4. *(Non–existence of non–constant steady state) Let μ_1 be the smallest positive eigenvalue of the operator $-\Delta$ on Ω with zero–flux boundary condition. Under Assumption 1, let D_2 be a fixed positive constant satisfying $D_2 > \frac{s(c-q)}{\mu_1}$. Then there exists a positive constant $D_1 = D_1(\Gamma, D_2)$ such that model (4) has no positive non–constant steady-state provided that $d_1 \ge D_1$, $d_2 \ge D_2$.*

Proof. Let $(N(x), P(x))$ be any positive solution of model (4) and denote $\bar{g} = |\Omega|^{-1}\int_\Omega g dx$. Then, multiplying the first equation of model (4) by $(N-\bar{N})$ integrating over Ω, we find

$$\begin{aligned} d_1\int_\Omega |\nabla(N-\bar{N})|^2dx &= \int_\Omega (N-\bar{N})N\left(r-\frac{rN}{K}-\frac{m}{N+b}-\frac{cP}{N+a}\right)dx\\ &= \int_\Omega (N-\bar{N})^2\left(r-\frac{r}{K}(N+\bar{N})-\frac{bm}{(\bar{N}+b)(N+b)}\right.\\ &\quad \left.-\frac{acP}{(\bar{N}+a)(N+a)}\right)dx-\frac{c\bar{N}}{\bar{N}+a}\int_\Omega (N-\bar{N})(P-\bar{P})dx,\\ &\leq r\int_\Omega (N-\bar{N})^2+c\int_\Omega |N-\bar{N}||P-\bar{P}|dx. \end{aligned} \tag{32}$$

In a similar manner, multiplying the second equation in model (4) by $(P-\bar{P})$ and from Theorem 4.3, we have

$$\begin{aligned} & d_2\int_\Omega |\nabla(P-\bar{P})|^2dx\\ &= \int_\Omega s(P-\bar{P})P\left(-q-\delta P+\frac{cN}{N+a}\right)Pdx\\ &= \int_\Omega s(P-\bar{P})^2\left(\frac{c\bar{N}}{\bar{N}+a}-q-\delta(P+\bar{P})\right)dx\\ &\quad +\int_\Omega \frac{acsP}{(\bar{N}+a)(N+a)}(\bar{N}-N)(P-\bar{P})dx\\ &\leq s(c-q)\int_\Omega (P-\bar{P})^2dx+\int_\Omega \frac{acsP}{(\bar{N}+a)(N+a)}|\bar{N}-N||P-\bar{P}|dx\\ &\leq s(c-q)\int_\Omega (P-\bar{P})^2dx+\tilde{L}\int_\Omega |\bar{N}-N||P-\bar{P}|dx, \end{aligned} \tag{33}$$

where the positive constant $\tilde{L}$ dependent on Θ.

It follows from (32), (33) and the ε-Young Inequality that

$$\begin{aligned} & d_1\int_\Omega |\nabla(N-\bar{N})|^2dx+d_2\int_\Omega |\nabla(P-\bar{P})|^2dx\\ &\leq \int_\Omega \left(r(N-\bar{N})^2+s(c-q)(P-\bar{P})^2\right)dx+2L\int_\Omega |\bar{N}-N||P-\bar{P}|dx\\ &\leq \int_\Omega \left(\left(r+\frac{L}{\varepsilon}\right)(N-\bar{N})^2+\left(s(c-q)+\varepsilon L\right)(P-\bar{P})^2\right)dx \end{aligned} \tag{34}$$

for $L=\dfrac{\tilde{L}+c}{2}$ and an arbitrary positive constant ε. It follows from the well–known Poincaré inequality that

$$\begin{aligned} & d_1\int_\Omega |\nabla(N-\bar{N})|^2dx+d_2\int_\Omega |\nabla(P-\bar{P})|^2dx\\ &\leq \frac{1}{\mu_1}\left(\left(r+\frac{L}{\varepsilon}\right)\int_\Omega |\nabla(N-\bar{N})|^2dx+\left(s(c-q)+\varepsilon L\right)\int_\Omega |\nabla(P-\bar{P})|^2dx\right). \end{aligned}$$

Since $d_2\mu_1 > s(c-q)$ from the assumption, we can find a sufficiently small ε such that $d_2\mu_1 \geq s(c-q)+\varepsilon L$. Finally, by taking $D_1 := \dfrac{1}{\mu_1}\left(r+\dfrac{L}{\varepsilon}\right)$, one can conclude that $N=\bar{N}$ and $P=\bar{P}$, which asserts our results. $\square$

4.3. Existence of non–constant positive steady states. In this subsection, we shall discuss the existence of the positive non–constant solution of model (4). We denote $\mathbf{w}^* = E^*$. Unless otherwise specified, in the following section, we always require that *Assumption 2* holds.

Let $\mathbf{X}$ be the space defined in (12) and let

$$\mathbf{X}^+ = \{(N,\, P) \in \mathbf{X} |\ N,\, P > 0 \ \text{ on } \ \bar{\Omega}\}.$$

We rewrite model (4) in the form:

$$\begin{cases} -\Delta \mathbf{w} = \mathbf{G}(\mathbf{w}), & \mathbf{w} \in \mathbf{X}^+, \\ \partial_{\mathbf{n}} \mathbf{w} = 0 & \text{on } \partial\Omega, \end{cases} \tag{35}$$

where

$$\mathbf{G}(\mathbf{w}) = \begin{pmatrix} \dfrac{N}{d_1}\left(r - \dfrac{r}{K}N - \dfrac{m}{N+b} - \dfrac{cP}{N+a}\right) \\ \dfrac{sP}{d_2}\left(-q - \delta P + \dfrac{cN}{N+a}\right) \end{pmatrix}.$$

Define a compact operator $\mathcal{F} : \mathbf{X}^+ \to \mathbf{X}^+$ by

$$\mathcal{F}(\mathbf{w}) := (\mathbf{I} - \Delta)^{-1}\{\mathbf{G}(\mathbf{w}) + \mathbf{w}\},$$

where $(\mathbf{I}-\Delta)^{-1}$ is the inverse operator of $\mathbf{I}-\Delta$ subject to the zero–flux boundary condition. Then $\mathbf{w}$ is a positive solution of model (35) if and only if $\mathbf{w}$ satisfies

$$(\mathbf{I} - \mathcal{F})\mathbf{w} = 0, \ \text{ in } \mathbf{X}^+.$$

To apply the index theory, we investigate the eigenvalue of the problem

$$-\left(\mathbf{I} - \mathcal{F}_{\mathbf{w}}(\mathbf{w}^*)\right)\Psi = \lambda\Psi, \ \Psi \neq \mathbf{0}, \tag{36}$$

where $\Psi = (\Psi_1, \Psi_2)^T$ and $\mathcal{F}_{\mathbf{w}}(\mathbf{w}^*) = (\mathbf{I}-\Delta)^{-1}(\mathbf{I}+\mathbf{A})$ with

$$\begin{aligned} \mathbf{A} &= \begin{pmatrix} \dfrac{1}{d_1}\left(N^*\left(\dfrac{m}{(N^*+b)^2} - \dfrac{r}{K}\right) + \dfrac{cN^*P^*}{(a+N^*)^2}\right) & -\dfrac{cN^*}{d_1(a+N^*)} \\ \dfrac{acsP^*}{d_2(a+N^*)^2} & -\dfrac{s\delta P^*}{d_2} \end{pmatrix} \\ &:= \begin{pmatrix} d_1^{-1}a_1 & -d_1^{-1}a_2 \\ d_2^{-1}a_3 & -d_2^{-1}a_4 \end{pmatrix}. \end{aligned}$$

In fact, after calculation, (36) can be rewritten as

$$\begin{cases} -(\lambda+1)\Delta\Psi + (\lambda\mathbf{I} - \mathbf{A})\Psi = 0, & x \in \Omega, \\ \partial_{\mathbf{n}}\Psi = 0, & x \in \partial\Omega, \\ \Psi \neq 0. \end{cases} \tag{37}$$

Observe that (37) has a non–trivial solution if and only if $\mathrm{Det}(\lambda\mathbf{I} + (\mu_i+1)^{-1}(\mu_i\mathbf{I} - \mathbf{A})) = 0$ for some $\lambda \geq 0$ and $i \geq 0$. That is to say, λ is an eigenvalue of (36), and so (37), if and only if $-\lambda$ is an eigenvalue of the matrix $(\mu_i+1)^{-1}(\mu_i\mathbf{I}-\mathbf{A})$ for any $i\geq 0$. Therefore, If $\mathbf{I}-\mathcal{F}_{\mathbf{w}}(\mathbf{w}^*)$ is invertible, if and only if, for any $i\geq 0$ the matrix

$$M_i := \mu_i\mathbf{I}-\mathbf{A} = \begin{pmatrix} \mu_i - d_1^{-1}a_1 & d_1^{-1}a_2 \\ -d_2^{-1}a_3 & \mu_i + d_2^{-1}a_4 \end{pmatrix}$$

is invertible. A straightforward computation yields:

$$\mathrm{Det}(M_i) = d_1^{-1}d_2^{-1}\big(d_1d_2\mu_i^2 + (d_1a_4-d_2a_1)\mu_i + a_2a_3 - a_1a_4\big). \tag{38}$$

For the sake of convenience, we denote

$$H(d_1,d_2,\mu_i) = d_1d_2\mu_i^2 + (d_1a_4-d_2a_1)\mu_i + a_2a_3 - a_1a_4.$$

Then $H(d_1,d_2,\mu_i) = d_1d_2\mathrm{Det}(M_i)$.

If $(d_1a_4-d_2a_1)^2 > 4d_1d_2(a_2a_3-a_1a_4)$, then $H(d_1,d_2,\mu_i)=0$ has two real roots $\mu^{\pm}$ given by

$$\mu^+(d_1,d_2) = \frac{1}{2d_1d_2}\left(d_2a_1 - d_1a_4 + \sqrt{(d_1a_4-d_2a_1)^2 - 4d_1d_2(a_2a_3-a_1a_4)}\right),$$
$$\mu^-(d_1,d_2) = \frac{1}{2d_1d_2}\left(d_2a_1 - d_1a_4 - \sqrt{(d_1a_4-d_2a_1)^2 - 4d_1d_2(a_2a_3-a_1a_4)}\right).$$

Set

$$B := B(d_1,d_2) = \{\mu : \mu\geq 0, \mu^-(d_1,d_2) < \mu < \mu^+(d_1,d_2)\},$$

$$S_p = \{\mu_0,\mu_1,\mu_2,\cdots\},$$

where $m(\mu_i)$ is the multiplicity of μ_i.

To compute index$(\mathbf{I}-\mathcal{F},\mathbf{w}^*)$, we can assert the following conclusion by Pang and Wang [56]:

Lemma 4.5. *([56]) Suppose $H(d_1,d_2,\mu_i)\neq 0$ for all $\mu_i\in S_p$. Then*

$$\textit{index}(\mathbf{I}-\mathcal{F},\mathbf{w}^*) = (-1)^{\sigma},$$

where

$$\sigma = \begin{cases} \displaystyle\sum_{\mu_i\in B\cap S_p} m(u_i), & \text{if } B\cap S_p\neq\emptyset, \\ 0, & \text{if } B\cap S_p = \emptyset. \end{cases}$$

In particular, if $H(d_1,d_2,\mu_i) > 0$ for all $\mu\geq 0$, then $\sigma = 0$.

From Lemma 4.5, if we want to calculate the index of index$(\mathbf{I}-\mathcal{F},\mathbf{w}^*)$, the key step is to determine the range of μ_i for which $H(d_1,d_2,\mu_i)<0$. For the proof of this, we need the following assumption.

Assumption 3.

(a) $s < \dfrac{d_2cN^*A(N^*)}{d_1\delta(a+N^*)^2g(N^*)}$;

(b)

$$\frac{N^*A(N^*)}{d_1(a+N^*)} - \frac{s\delta(a+N^*)g(N^*)}{cd_2} > 2\sqrt{-\frac{sN^*g(N^*)}{d_1d_2c(a+N^*)^2}\Big(\delta(a+N^*)^2)A(N^*) - ac^2\Big)},$$

where $A(N^*) = (a+N^*)g'(N^*) + g(N^*)$

Theorem 4.6. *(Existence of non–constant steady state) Under the conditions of Theorem 4.3 and Assumption 3, if* $\mu^- \in (\mu_i,\, \mu_{i+1})$ *and* $\mu^+ \in (\mu_j,\, \mu_{j+1})$ *for some* $0 \le i < j$*, and* $\displaystyle\sum_{k=i+1}^{j} m(u_k)$ *is odd, then model (4) has at least one non–constant solution.*

Proof. Since *Assumption 3*, equivalently, $(d_1a_4 - d_2a_1)^2 > 4d_1d_2(a_2a_3 - a_1a_4)$, it follows that $\mu^{\pm}$ exists. On the contrary, suppose that model (4) has no non–constant positive solution. By Theorem 4.4, we can fixed $\bar{d}_1 > d_1$ and $\bar{d}_2 > d_2$ such that

(i) model (4) with diffusion coefficients $\bar{d}_1$ and $\bar{d}_2$ has no non–constant solutions;
(ii) $H(\bar{d}_1, \bar{d}_2, \mu_i) > 0$ for all $\mu \ge 0$.

By virtue of Theorem 4.3, there exists a positive constant $C = C(\Gamma)$ such that for and $\tilde{D}_1 \ge d_1, \tilde{D}_2 \ge d_2$, any solution (N, P) of model (4) with diffusion coefficients $\tilde{D}_1$ and $\tilde{D}_2$ satisfies $C^{-1} < N,\, P < C, x \in \bar{\Omega}$.

Set

$$\mathcal{M} = \left\{(N,\ P) \in C(\overline{\Omega}) \times C(\overline{\Omega}) : C^{-1} < N,\ P < C \ \text{ in } \ \overline{\Omega})\right\},$$

and define

$$\Phi :\ \mathcal{M} \times [0,\, 1] \to C(\overline{\Omega}) \times C(\overline{\Omega})$$

by

$$\Phi(\mathbf{w},\, \theta) = (\mathbf{I} - \Delta)^{-1}\{\mathbf{G}(\mathbf{w},\, \theta) + \mathbf{w}\},$$

where

$$\mathbf{G}(\mathbf{w},\, \theta) = \begin{pmatrix} \left(\theta d_1 + (1-\theta)\bar{d}_1\right)^{-1} \cdot N\left(r - \dfrac{r}{K}N - \dfrac{m}{N+b} - \dfrac{cP}{N+a}\right) \\ \left(\theta d_2 + (1-\theta)\bar{d}_2\right)^{-1} \cdot sP\left(-q - \delta P + \dfrac{cN}{N+a}\right) \end{pmatrix}.$$

It is clear that finding the positive solution of model (35) becomes equivalent to finding the fixed point of $\Phi(\mathbf{w},\, 1)$ in $\mathcal{M}$. Further, by virtue of the definition of $\mathcal{M}$, we have that $\Phi(\mathbf{w},\, \theta) = 0$ has no fixed point in $\partial\mathcal{M}$ for all $0 \le \theta \le 1$.

Since $\Phi(\mathbf{w},\, t)$ is compact, the Leray–Schauder topological degree

$$\deg(\mathbf{I} - \Phi(\mathbf{w}, \theta), \mathcal{M}, 0)$$

is well defined. From the invariance of Leray–Schauder degree at the homotopy, we deduce

$$\deg(\mathbf{I} - \Phi(\mathbf{w},\, 1),\, \mathcal{M},\ 0) = \deg(\mathbf{I} - \Phi(\mathbf{w},\, 0),\, \mathcal{M},\ 0). \tag{39}$$

In view of $\mu^- \in (\mu_i,\, \mu_{i+1})$ and $\mu^+ \in (\mu_j,\, \mu_{j+1})$, we have $B(d_1, d_2) \cap S_p = \{\mu_{i+1}, \mu_{i+2}, \cdots, \mu_j\}$. Clearly, $\mathbf{I} - \Phi(\mathbf{w},\, 1) = \mathbf{I} - \mathcal{F}$. Thus, if model (4) has no other solutions except the constant one $\mathbf{w}^*$, then Lemma 4.5 shows that

$$\deg(\mathbf{I} - \Phi(\mathbf{w},\, 1),\, \mathcal{M},\ 0) = \operatorname{index}(\mathbf{I} - \mathcal{F},\, \mathbf{w}^*) = (-1)^{\sum_{k=i+1}^{j} m(u_k)} = -1. \tag{40}$$

On the contrary, by the choice of $\bar{d}_1$ and $\bar{d}_2$, and (ii) above, we have that $B(\bar{d}_1, \bar{d}_2) \cap S_p = \emptyset$ and $\mathbf{w}^*$ is the only fixed point of $\Phi(\mathbf{u},\, 0)$. It therefore follows from Lemma 4.5 that

$$\deg(\mathbf{I} - \Phi(\mathbf{w},\, 0),\, \mathcal{M},\ 0) = \operatorname{index}(\mathbf{I} - \mathcal{F},\, \mathbf{w}^*) = (-1)^0 = 1. \tag{41}$$

From (39)–(41), we get a contradiction. Therefore, there exists a non–constant solution of model (4). The proof is completed. ☐

One direct application of Theorem 4.6 is presented as the following corollary.

Corollary 1. *Under the conditions of Theorem 4.3, if* $a_1 > 0$, $\dfrac{a_1}{d_1} \in (\mu_j, \mu_{j+1})$ *for some* $j \geq 1$, *and* $\sum_{i=1}^{j} m(\mu_i)$ *is odd, then there exists a positive constant* d^* *such that model (4) has at least one non–constant solution if* $d_2 > d^*$.

Proof. Since $a_1 > 0$, it follows that if d_2 is large enough then $(d_1a_4 - d_2a_1)^2 > 4d_1d_2(a_2a_3 - a_1a_2)$ and $0 < \mu^-(d_1, d_2) < \mu^+(d_1, d_2)$. Furthermore,

$$\mu^-(d_1, d_2) \to 0, \ \mu^+(d_1, d_2) \to \frac{a_1}{d_1}, \quad \text{as} \quad d_2 \to \infty.$$

Since $\dfrac{a_1}{d_1} \in (\mu_j, \mu_{j+1})$ for some $j \geq 1$, there exists $d_0 \gg 1$ such that

$$\mu^+(d_1, d_2) \in (\mu_j, \mu_{j+1}), \ 0 < \mu^-(d_1, d_2) < \mu_1, \ \forall d_2 \geq d_0.$$

Therefore, for $d_2 > 0$ large, $\sum_{i=1}^{j} m(\mu_i)$ is odd which implies (i) and (ii) in Theorem 4.6. This concludes the proof. □

5. Turing instability and pattern formation.

In the previous section, we prove that there are non-constant positive steady states in model (1). In this section, we will focus on that, if the parameters are properly chosen, the non-constant positive steady states can give birth to Turing stationary patterns as a result of diffusion. First of all, we will give the conditions of Turing instability for model (1).

5.1. Turing instability.

In this subsection, we mainly focus on the conditions of Turing instability of the solutions to model (1) with weak Allee effect. Mathematically speaking, a positive constant steady state E^* is unstable due to Turing instability or diffusion–induced instability, which was emphasized by Turing in his pioneering work in 1952 [70], means that E^* is an asymptotically stable homogeneous steady state for the spatially homogeneous version of model (1) (i.e. $d_1 = d_2 = 0$) but is unstable for model (1). The instability arises due to the small heterogeneous perturbation around the homogeneous steady–state.

If the homogeneous steady-state of model (1) is unstable, then one of the eigenvalues of matrix $A_i = -\mu_i D + J$ has positive real part, which depends on the signs of trace and determinant of A_i:

$$\mathrm{Tr}(A_i) = -\mu_i(d_1 + d_2) + \mathrm{Tr}(J),$$

$$\mathrm{Det}(A_i) = d_1d_2\mu_i^2 - \left(d_2\left(N^*g'(N^*) + \frac{cN^*P^*}{(a+N^*)^2}\right) - d_1s\delta P^*\right)\mu_i + \mathrm{Det}(J).$$

According to the definition of the Turing instability, in the case without diffusion (i.e., $d_1 = d_2 = 0$), E^* is stable, then $\mathrm{Tr}(J) < 0$ and $\mathrm{Det}(J) > 0$ hold, thus $\mathrm{Tr}(A_i) < 0$ is always true. Hence if A_i has an eigenvalue with positive real part, then it must be a real value one and the other eigenvalue must be a negative real one. A necessary condition is

$$s < \frac{d_2cN^*(g(N^*) + (a+N^*)g'(N^*))}{d_1\delta(a+N^*)^2g(N^*)}.$$

Otherwise $\mathrm{Det}(A_i) > 0$ for all $\mu_i \geq 0$ since $\mathrm{Det}(J) > 0$. For the Turing instability, we need $\mathrm{Det}(A_i) < 0$ for some $\mu_i > 0$. Notice that $\mathrm{Det}(A_i)$ achieves its minimum:

$$\min_{\mu_i} \mathrm{Det}(A_i) = \frac{4d_1 d_2 \mathrm{Det}(J) - \left(d_2\left(N^* g'(N^*) + \dfrac{cN^*P^*}{(a+N^*)^2}\right) - d_1 s\delta P^*\right)^2}{4d_1 d_2}, \quad (42)$$

at the critical value $\mu^* > 0$ when

$$\mu^* = \frac{1}{2d_1 d_2}\left(d_2\left(N^* g'(N^*) + \frac{cN^*P^*}{(a+N^*)^2}\right) - d_1 s\delta P^*\right).$$

If Assumption 3 (a) holds and $\min\limits_{\mu_i} \mathrm{Det}(A_i) < 0$, then E^* is an unstable equilibrium with respect to model (1). Summarizing the above calculation, we conclude

Theorem 5.1. *(Turing instability) Under Assumptions 2 and 3, the positive constant steady state solution $E^* = (N^*, P^*)$ of model (1) with weak Allee effect is Turing unstable.*

Remark 4. In the case $\delta = 0$, i.e., without density dependent death rate for the predators in model (1), in view of the case without diffusion ($d_1 = d_2 = 0$), E^* of model (1) is stable, which means that $\mathrm{Tr}(J) < 0$ and $\mathrm{Det}(J) > 0$, and we can only obtain $\mathrm{Tr}(A_i) < 0$, $\mathrm{Det}(A_i) > 0$. As a consequence, there is no Turing instability in model (1) with $\delta = 0$ [21]. And in the case with the density dependent death rate $\delta > 0$, the term $-d_1 s\delta P^*$ in $\mathrm{Det}(A_i)$ can make $\mathrm{Det}(A_i) < 0$, which results in Turing instability. And Theorem 5.1 shows that the density dependent death rate for the predators may be one of the determining factors induced Turing instability in model (1), i.e., Turing patterns emerge. Biologically speaking, the density dependent death rate $\delta > 0$ has depressing effect on the growth rate of the predator, i.e., cause the reduction in predator growth rate. And a growing population has a greater abundance of young individuals whereas older individuals appear in greater numbers in an equilibrium population, and older individuals are more likely to have lower intrinsic mortality [68].

5.2. Pattern formation.

In this section, we mainly answer our proposed questions 2 in the introduction via numerical simulations. All our numerical simulations employ the zero–flux boundary conditions and within a spatial domain of size 100×100 (the lattice size). The numerical integration of model (1) is performed by using a finite difference approximation for the spatial derivatives and an explicit Euler method for the time integration [28] with a time step size of $1/100$. The initial condition is always a small amplitude random perturbation around the positive constant steady state solution $E^* = (N^*, P^*)$ of model (1). After the initial period during which the perturbation spread, either the model goes into a time dependent state, or to an essentially steady state solution (time independent).

In the numerical simulations, different types of dynamics are observed and it is found that the distributions of predator and prey are always of the same type. Consequently, we can restrict our analysis of pattern formation to one distribution. In this section, we show the distribution of prey N, for instance. We have taken some snapshots with red (blue) corresponding to the high (low) value of prey N.

Now, we show the Turing pattern for the different values of the parameters. Via numerical simulation, one can see that the model dynamics exhibits spatiotemporal complexity of pattern formation, including hot spots, stripes and cold spots Turing patterns.

In the numerical simulations, the following parameters are fixed as

$$r = 1,\ K = 10,\ m = 0.1,\ b = 0.9,\ c = 1,\ q = 0.35,\ \delta = 0.0425,\ d_1 = 0.015,\ d_2 = 1. \tag{43}$$

First, we choose $(a, s) = (1.5,\ 3)$. Note that

$$\begin{aligned}
&3 = s > \frac{cN^*(g(N^*) + (a + N^*)g'(N^*))}{\delta(a + N^*)^2 g(N^*)} = 2.8990,\\
&3 < \frac{d_2 cN^*(g(N^*) + (a + N^*)g'(N^*))}{d_1\delta(a + N^*)^2 g(N^*)} = 193.264,\\
&\mathrm{Det}(J) = 0.5370,\ \mathrm{Tr}(\mathbf{A})^2 - 4\mathrm{Det}(\mathbf{A}) = 0.0423 > 0,
\end{aligned}$$

then we can conclude, from Theorem 5.1, that the positive constant steady state solution $E^* = (N^*,\ P^*) = (1.2056, 2.2512)$ of model (1) is Turing unstable.

In Fig. 2, we show the time process of spots pattern formation of the prey N at $t = 0, 100, 3000$ for the parameters as (43) and $(a, s) = (1.5,\ 3)$. In this case, there exhibits a competition between stripes and spots. The pattern takes a long time to settle down, starting with a homogeneous state $E^* = (1.2056, 2.2512)$ (c.f., Fig. 2(a)), the random perturbations lead to the formation of stripes and spots (c.f., Fig. 2(b)), and the later random perturbations make these stripes decay, and ending with the time–independent regular spots pattern (c.f., Fig. 2(c)), which is isolated zones with low prey densities, and we call this pattern as hot spots pattern. Ecologically, hot spots pattern shows that the prey population are driven by predators to a very high level in those regions. The final result is the formation of patches of high prey density surrounded by areas of low prey densities. That's to say, under the control of these parameters, the prey is predominant in the area.

When changing the value of (a, s) to $(2,\ 2.2)$, and keep other parameters unchange, we have

$$\begin{aligned}
&2.2 = s > \frac{cN^*(g(N^*) + (a + N^*)g'(N^*))}{\delta(a + N^*)^2 g(N^*)} = 1.6918,\\
&2.2 < \frac{d_2 cN^*(g(N^*) + (a + N^*)g'(N^*))}{d_1\delta(a + N^*)^2 g(N^*)} = 112.785,\\
&\mathrm{Det}(J) = 0.3687,\ \mathrm{Tr}(\mathbf{A})^2 - 4\mathrm{Det}(\mathbf{A}) = 0.0222 > 0.
\end{aligned}$$

In this case, from Theorem 5.1, we can know that Turing instability emerges, and we can obtain the stationary stripes pattern, c.f., Fig. 3.

While choosing $(a, s) = (2.5, 1.5)$, we have

$$\begin{aligned}
&1.5 = s > \frac{cN^*(g(N^*) + (a + N^*)g'(N^*))}{\delta(a + N^*)^2 g(N^*)} = 0.8412,\\
&1.5 < \frac{d_2 cN^*(g(N^*) + (a + N^*)g'(N^*))}{d_1\delta(a + N^*)^2 g(N^*)} = 56.08,\\
&\mathrm{Det}(J) = 0.2393,\ \mathrm{Tr}(\mathbf{A})^2 - 4\mathrm{Det}(\mathbf{A}) = 0.0014 > 0.
\end{aligned}$$

The conditions of Theorem 5.1 hold and $E^* = (1.8233,\ 2.9858)$ is Turing unstable. Via numerical simulation, we can obtain the stationary cold spots pattern, c.f., Fig. 4.

Comparing Fig. 4 with Fig. 2(c), we find that they share similarities. Fig. 2(c) consists of red (maximum density of N) spots on a blue (minimum density of N) background, i.e., the preys are isolated zones with high population density. While in Fig. 4 consists of blue (minimum density of N) spots on a red (maximum density of N) background, i.e., the preys are isolated zones with low population density.

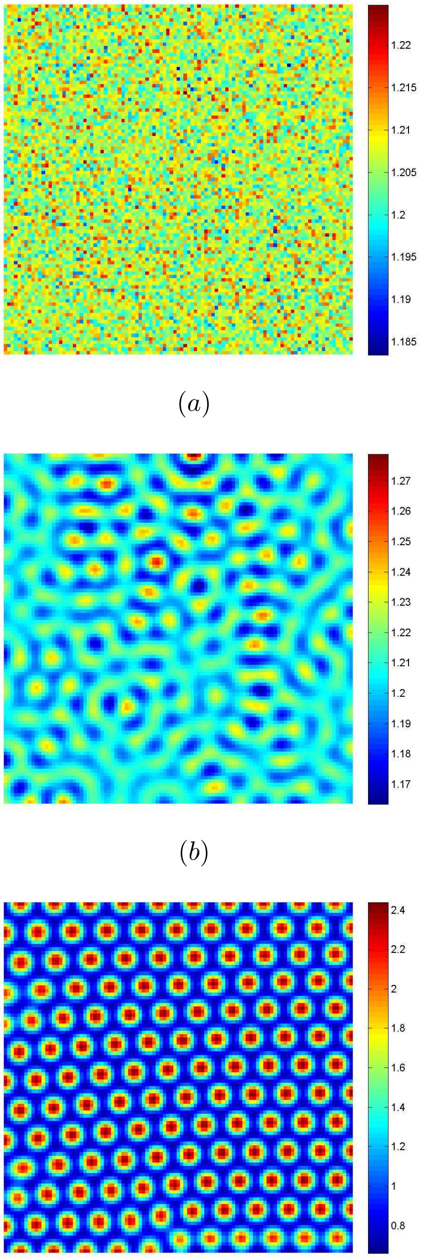

(a)

(b)

(c)

Figure 2. Stationary hot spots pattern in model (1). The parameter values are taken as (43) and $(a, s) = (1.5,\ 3)$. The zero-flux boundary condition is used and initial condition is small perturbation around the homogeneous steady-state $E^{*} = (1.2056, 2.2512)$.

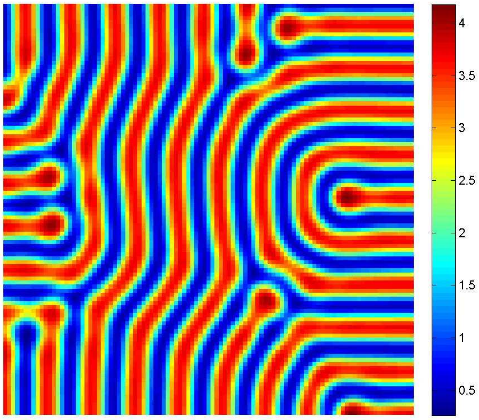

FIGURE 3. Stationary stripes pattern in model (1) with parameter values as (43) and $(a, s) = (2,\ 2.2)$. The zero-flux boundary condition is used and initial condition is small perturbation around the homogeneous steady-state $E^* = (1.8233,\ 2.9858)$.

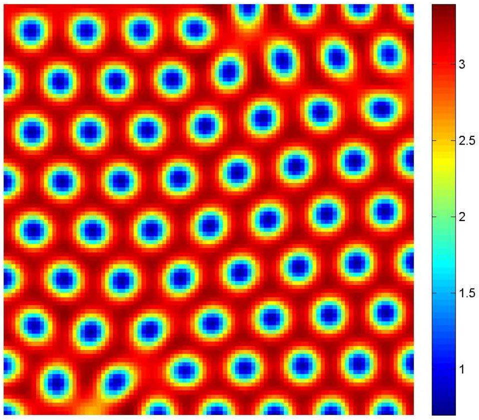

FIGURE 4. Stationary cold spots pattern in model (1) with parameter values as (43) and $(a, s) = (2.5,\ 1.5)$. The zero-flux boundary condition is used and initial condition is small perturbation around the homogeneous steady-state $E^* = (2.5354, 3.6122)$.

6. **Conclusions and remarks.** Dynamical complexity of spatiotemporal model of a prey-predator model with weak Allee effects in the prey growth and density dependent death rate of predator is thoroughly investigated in this paper. Here we have obtained the lower and upper bounds of time-dependent solutions of the coupled nonlinear partial differential equations with Neumann boundary condition.

Derivation of the bounds along with certain parametric restrictions lead to the persistence condition of both species at all future time (c.f., Theorem 3.3). We have derived the local and global stability conditions for all possible homogeneous steady-states involved with the model (c.f., Theorems 3.4 and 3.6). Stability of the homogeneous steady-states are dependent upon the parametric restrictions. The conditions obtained for the local and global stability of constant coexistence steady-state are implicit conditions as the components of the steady-state can not be found explicitly. Coexistence steady-state loses stability through Hopf bifurcation (c.f., Theorem 3.7). Complicated analytical conditions for stability of extinction steady-state and coexistence steady-state prevent us to comment about the possibility of having bistable scenario.

Apart from the constant steady-state the model under consideration also admits non-constant steady-state. Existence of non-constant steady-state depends upon certain parametric restrictions involving intrinsic rate constants and rate of diffusivity of prey and predator species (c.f., Theorem 4.6). The conditions we have derived here are unable to determine the boundaries in the parametric domain where we find non-uniform distribution of two species over their habitat as the relevant conditions are highly implicit. The implicit conditions prevent us to understand the most sensitive parameter towards the generation of non-constant steady-states.

Biologically, we partially provide answers to the two questions proposed in the introduction: What is the effect of density dependent death rate for the predator on the spatiotemporal dynamics of our model? How many stationary Turing patterns may there be in our model? We summarize our main findings as follows:

1. **Density dependent death rate can induce Turing instability**: When $\delta = 0$, model (1) without density dependent death rate for the predator, there is no Turing instability. From Theorem 5.1, one can know that the positive constant steady state $E^* = (N^*, P^*)$ of model (1) with weak Allee effect is Turing unstable. That's to say, density dependent death rate for the predator is the determining factors induced Turing instability in the model. In this case, despite that the solutions are stable, the diffusion can de-stabilize the symmetric solutions so that the system with diffusion added can have the symmetry-breaking capabilities, i.e., form the stationary Turing pattern.
2. **The model dynamics exhibits rich and complex pattern formation:** Via numerical simulations in Figures 2, 3 and 4, we find that the model dynamics exhibits formation growth to hot spots (i.e, Fig. 2), stripes (i.e, Fig. 3) and cold spots (i.e, Fig. 4) pattern replication. This shows that the pattern formation of the model (1) is not simple, but rich and complex.

REFERENCES

[1] P. A. Abrams, The fallacies of "ratio-dependent" predation, *Ecology*, **75** (1994), 1842–1850.

[2] P. A. Abrams and L. R. Ginzburg, The nature of predation: prey dependent, ratio dependent or neither?, *Trends in Ecology & Evolution*, **15** (2000), 337–341.

[3] P. Aguirre, E. González-Olivares and E. Sáez, Two limit cycles in a Leslie-Gower predator-prey model with additive Allee effect, *Nonlinear Analysis: Real World Applications*, **10** (2009), 1401–1416.

[4] P. Aguirre, E. González-Olivares and E. Sáez, Three limit cycles in a Leslie-Gower predator-prey model with additive Allee effect, *SIAM Journal on Applied Mathematics*, **69** (2009), 1244–1262.

[5] H. R. Akçakaya, R. Arditi and L. R. Ginzburg, Ratio-dependent predation: An abstraction that works, *Ecology*, **76** (1995), 995–1004.

[6] N. D. Alikakos, An application of the invariance principle to reaction-diffusion equations, *Journal of Differential Equations*, **33** (1979), 201–225.

[7] W. C. Allee, *Animal Aggregations, a Study in General Sociology*, University of Chicago Press, Chicago, USA, 1931.

[8] D. Alonso, F. Bartumeus and J. Catalan, Mutual interference between predators can give rise to Turing spatial patterns, *Ecology*, **83** (2002), 28–34.

[9] R. Arditi and L. R. Ginzburg, Coupling in predator-prey dynamics: Ratio-dependence, *Journal of Theoretical Biology*, **139** (1989), 311–326.

[10] A. Ardito and P. Ricciardi, Lyapunov functions for a generalized Gause-type model, *Journal of Mathematical Biology*, **33** (1995), 816–828.

[11] M. Banerjee and S. Banerjee, Turing instabilities and spatio-temporal chaos in ratio-dependent Holling-Tanner model, *Mathematical Biosciences*, **236** (2012), 64–76.

[12] M. Banerjee and S. Petrovskii, Self-organized spatial patterns and chaos in a ratio-dependent predator-prey system, *Theoretical Ecology*, **4** (2011), 37–53.

[13] M. Baurmann, T. Gross and U. Feudel, Instabilities in spatially extended predator–prey systems: Spatio-temporal patterns in the neighborhood of Turing-Hopf bifurcations, *Journal of Theoretical Biology*, **245** (2007), 220–229.

[14] D. L. Benson, J. A. Sherratt and P. K. Maini, Diffusion driven instability in an inhomogeneous domain, *Bulletin of Mathematical Biology*, **55** (1993), 365–384.

[15] A. A. Berryman, The orgins and evolution of predator-prey theory, *Ecology*, **73** (1992), 1530–1535.

[16] C. Bianca, Existence of stationary solutions in kinetic models with Gaussian thermostats, *Mathematical Methods in the Applied Sciences*, **36** (2013), 1768–1775.

[17] D S Boukal and L. Berec, Single-species models of the Allee effect: Extinction boundaries, sex ratios and mate encounters, *Journal of Theoretical Biology*, **218** (2002), 375–394.

[18] D. S. Boukal, M. W. Sabelis and L. Berec, How predator functional responses and Allee effects in prey affect the paradox of enrichment and population collapses, *Theoretical Population Biology*, **72** (2007), 136–147.

[19] N. F. Britton, *Essential Mathematical Biology*, Springer, 2003.

[20] K. J. Brown, P. C. Dunne and R. A. Gardner, A semilinear parabolic system arising in the theory of superconductivity, *Journal of Differential Equations*, **40** (1981), 232–252.

[21] Y. Cai, W. Wang and J. Wang, Dynamics of a diffusive predator–prey model with additive Allee effect, *International Journal of Biomathematics*, **5** (2012), 1250023, 11 pp.

[22] R. S. Cantrell and C. Cosner, *Spatial Ecology via Reaction-Diffusion Equations*, Wiley, London, 2003.

[23] E. Conway, D. Hoff and J. Smoller, Large time behavior of solutions of systems of nonlinear reaction-diffusion equations, *SIAM Journal of Appllied Mathematics*, **35** (1978), 1–16.

[24] L. B. Crowder and W. E. Cooper, Habitat structural complexity and the interaction between bluegills and their prey, *Ecology*, **63** (1982), 1802–1813.

[25] B. Dennis, Allee effects: Population growth, critical density, and the chance of extinction, *Natural Resource Modeling*, **3** (1989), 481–538.

[26] X. Ding and J. Jiang, Positive periodic solutions in delayed Gause-type predator-prey systems, *Journal of Mathematical Analysis and Applications*, **339** (2008), 1220–1230.

[27] K. Fujii, Complexity-stability relationship of two-prey-one-predator species system model: Local and global stability, *Journal of Theoretical Biology*, **69** (1977), 613–623.

[28] M. R. Garvie, Finite-difference schemes for reaction-diffusion equations modeling predator-prey interactions in Matlab, *Bulletin of Mathematical Biology*, **69** (2007), 931–956.

[29] D. Gilbarg and N. S. Trudinger, *Elliptic Partial Differential Equations of Second Order*, Springer-Verlag, Berlin and New York, 1983.

[30] E. González-Olivares, H. Meneses-Alcay, B. González-Yañez, J. Mena-Lorca, A. Rojas-Palma and R. Ramos-Jiliberto, Multiple stability and uniqueness of the limit cycle in a Gause-type predator–prey model considering the allee effect on prey, *Nonlinear Analysis: Real World Applications*, **12** (2011), 2931–2942.

[31] K. Hasík, On a predator–prey system of Gause type, *Journal of Mathematical Biology*, **60** (2010), 59–74.

[32] D. Henry and D. B. Henry, *Geometric Theory of Semilinear Parabolic Equations*, Lecture Notes in Mathematics, 840, Springer-Verlag, Berlin-New York, 1981.

[33] S.-B. Hsu, T.-W. Hwang and Y. Kuang, Global analysis of the Michaelis-Menten-type ratio-dependent predator-prey system, *Journal of Mathematical Biology*, **42** (2001), 489–506.

[34] T.-W. Hwang, Uniqueness of the limit cycle for Gause-type predator-prey systems, *Journal of Mathematical Analysis and Applications*, **238** (1999), 179–195.

[35] Y. Kang and L. Wedekin, Dynamics of a intraguild predation model with generalist or specialist predator, *Journal of Mathematical Biology*, **67** (2013), 1227–1259.

[36] W. Ko and K. Ryu, A qualitative study on general Gause-type predator-prey models with constant diffusion rates, *Journal of Mathematical Analysis and Applications*, **344** (2008), 217–230.

[37] Y. Kuang, Global stability of Gause-type predator-prey systems, *Journal of Mathematical Biology*, **28** (1990), 463–474.

[38] Y. Kuang, Rich dynamics of Gause-type ratio-dependent predator-prey system, *Fields Institute Communication*, **21** (1999), 325–337.

[39] Y. Kuang and E. Beretta, Global qualitative analysis of a ratio-dependent predator-prey system, *Journal of Mathematical Biology*, **36** (1998), 389–406.

[40] Y. Kuang and H. I. Freedman, Uniqueness of limit cycles in Gause-type models of predator-prey systems, *Mathematical Biosciences*, **88** (1988), 67–84.

[41] S. A. Levin, The problem of pattern and scale in ecology, *Ecology*, **73** (1992), 1943–1967.

[42] M. A. Lewis and P. Kareiva, Allee dynamics and the spread of invading organisms, *Theoretical Population Biology*, **43** (1993), 141–158.

[43] C.-S. Lin, W.-M. Ni and I. Takagi, Large amplitude stationary solutions to a chemotaxis system, *Journal of Differential Equations*, **72** (1988), 1–27.

[44] Y. Liu, Geometric criteria for the nonexistence of cycles in Gause-type predator-prey systems, *Proceedings of the American Mathematical Society*, **133** (2005), 3619–3626.

[45] Y. Lou and W.-M. Ni, Diffusion, self-diffusion and cross-diffusion, *Journal of Differential Equations*, **131** (1996), 79–131.

[46] A. B. Medvinsky, S. V. Petrovskii, I. A. Tikhonova, H. Malchow and B.-L. Li, Spatiotemporal complexity of plankton and fish dynamics, *SIAM Review*, **44** (2002), 311–370.

[47] Z. Mei, *Numerical Bifurcation Analysis for Reaction-Diffusion Equations*, Springer, 2000.

[48] S. M. Moghadas and M. E. Alexander, Dynamics of a generalized Gause-type predator-prey model with a seasonal functional response, *Chaos, Solitons & Fractals*, **23** (2005), 55–65.

[49] S. M. Moghadas, M. E. Alexander and B. D. Corbett, A non-standard numerical scheme for a generalized Gause-type predator-prey model, *Physica D: Nonlinear Phenomena*, **188** (2004), 134–151.

[50] S. M. Moghadas and B. D. Corbett, Limit cycles in a generalized Gause-type predator-prey model, *Chaos, Solitons & Fractals*, **37** (2008), 1343–1355.

[51] A. Morozov and S. Petrovskii, Excitable population dynamics, biological control failure, and spatiotemporal pattern formation in a model ecosystem, *Bulletin of Mathematical Biology*, **71** (2009), 863–887.

[52] A. Morozov, S. Petrovskii and B.-L. Li, Bifurcations and chaos in a predator-prey system with the Allee effect, *Proceedings of the Royal Society of London-B: Biological Sciences*, **271** (2004), 1407–1414.

[53] J. D. Murray, Discussion: Turing's theory of morphogenesis–its influence on modelling biological pattern and form, *Bulletin of Mathematical Biology*, **52** (1990), 119–152.

[54] J. D. Murray, *Mathematical Biology*, Springer, New York, USA, 2002.

[55] C. Neuhauser, Mathematical challenges in spatial ecology, *Notices of the AMS*, **48** (2001), 1304–1314.

[56] P. Y. H. Pang and M. Wang, Qualitative analysis of a ratio-dependent predator-prey system with diffusion, *Proceedings of the Royal Society of Edinburgh-A-Mathematics*, **133** (2003), 919–942.

[57] P. Y. H. Pang and M. Wang, Strategy and stationary pattern in a three-species predator–prey model, *Journal of Differential Equations*, **200** (2004), 245–273.

[58] R. Peng and J. Shi, Non-existence of non-constant positive steady states of two Holling type-II predator-prey systems: Strong interaction case, *Journal of Differential Equations*, **247** (2009), 866–886.

[59] R. Peng, J. Shi and M. Wang, Stationary pattern of a ratio-dependent food chain model with diffusion, *SIAM Journal on Applied Mathematics*, **67** (2007), 1479–1503.

[60] R. Peng, J. Shi and M. Wang, On stationary patterns of a reaction-diffusion model with autocatalysis and saturation law, *Nonlinearity*, **21** (2008), 1471.

[61] A. M. de Roos, E. McCauley and W. G. Wilson, Pattern formation and the spatial scale of interaction between predators and their prey, *Theoretical Population Biology*, **53** (1998), 108–130.

[62] J. F. Savino and R. A. Stein, Predator-prey interaction between largemouth bass and bluegills as influenced by simulated, submersed vegetation, *Transactions of the American Fisheries Society*, **111** (1982), 255–266.

[63] A. Sikder and A. B. Roy, Persistence of a generalized Gause-type two prey-two predator pair linked by competition, *Mathematical Biosciences*, **122** (1994), 1–23.

[64] J. Smoller, *Shock Waves and Reaction-Diffusion Equations*, Springer-Verlag, New York, 1994.

[65] R. A. Stein, Selective predation, optimal foraging, and the predator-prey interaction between fish and crayfish, *Ecology*, **58** (1977), 1237–1253.

[66] P. A. Stephens and W. J. Sutherland, Consequences of the Allee effect for behaviour, ecology and conservation, *Trends in Ecology & Evolution*, **14** (1999), 401–405.

[67] P. A. Stephens, W. J. Sutherland and R. P. Freckleton, What is the Allee effect?, *Oikos*, (1999), 185–190.

[68] J. P. Stover, B. E. Kendall and G. A. Fox, Demographic heterogeneity impacts density-dependent population dynamics, *Theoretical Ecology*, **5** (2012), 297–309.

[69] P. Turchin, *Complex Population Dynamics: A Theoretical/Empirical Synthesis*, Princeton University Press, 2003.

[70] A. M. Turing, The chemical basis of morphogenesis, *Philosophical Transactions of the Royal Society of London-B*, **237** (1952), 37–72.

[71] R. K. Upadhyay, V. Volpert and N. K. Thakur, Propagation of turing patterns in a plankton model, *Journal of Biological Dynamics*, **6** (2012), 524–538.

[72] J. Wang, J. Shi and J. Wei, Dynamics and pattern formation in a diffusive predator–prey system with strong Allee effect in prey, *Journal of Differential Equations*, **251** (2011), 1276–1304.

[73] M. Wang, *Nonlinear Partial Differential Equations of Parabolic Type*, Science Press, Beijing, 1993.

[74] M. Wang, Stationary patterns of strongly coupled prey–predator models, *Journal of Mathematical Analysis and Applications*, **292** (2004), 484–505.

[75] M. Wang, Stationary patterns for a prey-predator model with prey-dependent and ratio-dependent functional responses and diffusion, *Physica D*, **196** (2004), 172–192.

[76] M. Wang, Stationary patterns caused by cross-diffusion for a three-species prey-predator model, *Computers and Mathematics with Applications*, **52** (2006), 707–720.

[77] W. Wang, Q. Liu and Z. Jin, Spatiotemporal complexity of a ratio-dependent predator-prey system, *Physical Review E*, **75** (2007), 051913.

[78] W. Wang, L. Zhang, H. Wang and Z. Li, Pattern formation of a predator-prey system with Ivlev-type functional response, *Ecological Modelling*, **221** (2010), 131–140.

[79] Z. Wu, J. Yin and C. Wang, *Elliptic and Parabolic Equations*, World Scientific, 2006.

[80] D. Xiao and S. Ruan, Global analysis in a predator-prey system with nonmonotonic functional response, *SIAM Journal on Applied Mathematics*, **61** (2001), 1445–1472.

[81] R. Xu, M. A. J. Chaplain and F. A. Davidson, Global stability of a Lotka–Volterra type predator-prey model with stage structure and time delay, *Applied Mathematics and Computation*, **159** (2004), 863–880.

[82] S. Zhou, Y. Liu and G. Wang, The stability of predator-prey systems subject to the Allee effects, *Theoretical Population Biology*, **67** (2005), 23–31.

Received March 31, 2014; Accepted July 21, 2014.

E-mail address: `caiyongli06@163.com`
E-mail address: `malayb@iitk.ac.in`
E-mail address: `yun.kang@asu.edu`
E-mail address: `weimingwang2003@163.com`